



Universidad de La Laguna

FACULTAD DE FÍSICA

INSTALLATION OF A SOLAR
PUMP IN A RURAL VILLAGE
IN SENEGAL

Trabajo de Fin de Grado

Author: Pablo Pérez Parrilla

Tutors: Fernando Lahoz Zamarro, Benjamín González Díaz, Gloria Eguaras

Contents

1	Theoretical Framework	2
1.1	Introduction to Band Theory	2
1.2	Doping Semiconductors. <i>p-n</i> Junction	5
1.3	<i>p-n</i> Junctions under solar irradiation. Solar cells efficiency principles.	13
2	Solar Pump Installation	15
2.1	Contextualization of the Installation	15
2.2	Description of the Installation	16
3	Challenges of International Cooperation	20
4	References	21
5	Annexes	22

Abstract

The objective of this project is to model and calculate the installation of a solar pump in a rural village in Kolda, Senegal. First, the theoretical framework of semiconductor physics is established, including a mild introduction to band theory, semiconductor doping and p - n junction. Then, the modelling of the installation begins with a description of the village and the living conditions of its people to finish with the proper calculations, where it has been found that the best option is to install six panels of 350 W of rated power to fulfill the power needs of the farm. A comparison is carried out between the actual pump installed on the field and the better suiting pumps according to the calculations to find out that the model *SPE* 18 – 12 is reasonably similar to the real pump while fitting with the calculations. Lastly, a reflection on the importance of international cooperation and why this project in particular has the correct approach is carried out.

1 Theoretical Framework

1.1 Introduction to Band Theory

Since the very beginnings of quantum theory, the energy of electrons in an atom is characterized as a discrete set of possible states. These states are filled from lowest to highest energy and each level admits two electrons, each one with different spin states to fulfill Pauli's principle. One electron can hop from one state to another with higher energy absorbing a photon of energy equal to the gap between levels. It can also decay to a state with lower energy by emitting a photon.

When talking about solids, which have an immense amount of atoms, it makes no sense to consider the individual energy levels of the electrons; instead, we talk about bands of proximate energy states. The electrons lie in those bands according to their energy and the bands are considered as a whole. In the same way that electrons cannot have energies that do not match the energy levels in the atom, the gap between the bands is a forbidden region. However, if a certain band is not completely full, the electrons can move almost freely inside the band. The last occupied band in a solid is called valence band, while the lowest unoccupied band is called conduction band (Nelson, 2003). It is possible for the electrons to hop from one band to another if it is provided with enough energy to cross the band gap between them.

In these terms, one can characterize a solid via its band structure, namely how electrons arrange in the valence and conduction bands. If the last band is partially occupied, the electrons can hop from one state to another and create an electric current. If the band gap with the previous band is large enough, there will always be empty states for the electrons to fill and we say that the material is a conductor. If, on the contrary, the last band is full and the gap with the next empty band is large, then the electrons do not have the possibility to move

among states and the material is an insulator. Lastly, if the valence band is full and the conduction band is empty but they are sufficiently close in energy, it is possible for the electrons to jump to the conduction band, producing a small electric current. In that case the solid is a semiconductor, which are of interest in solar cell physics.

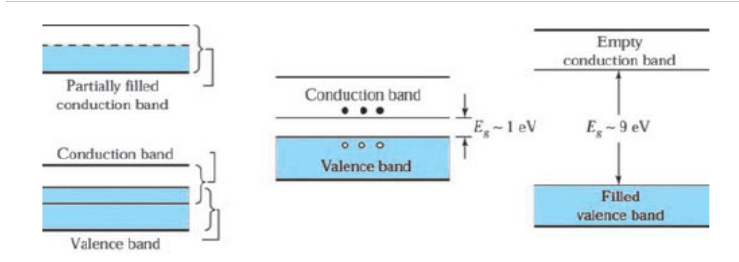


Figure 1: Classification of materials according to their band arrangement. (a) metal, (b) semiconductor and (c) insulator (Sze & Lee, 2012).

In general, semiconductors have band gaps between 0.5 eV to 4 eV (Nelson, 2003). This can happen through several processes, depending on the material. For instance, at room temperature, it is possible for the electrons to acquire enough kinetic energy due to a thermal excitation to cross the gap. There are also materials whose electrons can absorb photons coming from solar light and hop to the conduction band. This effect is called photoconductivity.

When an electron jumps from one band to the next one it leaves a hole in the valence band, which can be treated as a particle with positive charge. It is equivalent to characterize the process in terms of the movement of the electrons in the conduction band or the movement of the holes in the valence band.

Near the minimum of the conduction band it is convenient to make a parabolic approximation for the energy in terms of an effective mass. Assuming that the minimum is at $\vec{k} = \vec{k}_{min}$, the energy is given by:

$$E = E_{min} + \alpha |\vec{k} - \vec{k}_{min}|^2 + \dots \quad (1)$$

Then, we define the effective mass to be given by:

$$\frac{\hbar^2}{m_c^*} = \frac{\partial^2 E}{\partial k^2} \quad (2)$$

Accordingly, the energy can be approximated to:

$$E(\vec{k}) = E_{c0} + \frac{\hbar^2 |\vec{k} - \vec{k}_{min}|^2}{2m_c^*} \quad (3)$$

The effective mass defined here is chosen so that the dispersion at the bottom of the band is equal to the dispersion suffered by free electrons of mass m_c^* . It also describes how the electrons in the conduction band react when a force is applied. The energy equation can be used to obtain the electron velocity:

$$\vec{v} = \nabla_{\vec{k}} E(\vec{k}) = \frac{\hbar(\vec{k} - \vec{k}_{min})}{m_c^*} \quad (4)$$

An analogous calculation is carried out for the holes in the valence band. Considering the band maximum to be at $\vec{k} = \vec{k}_{max}$, the energy for the holes is:

$$E(\vec{k}) = E_{max} - \frac{\hbar^2 |\vec{k} - \vec{k}_{max}|^2}{2m_v^*} \quad (5)$$

Where the effective mass is defined to be always positive for the holes at the top of the valence band:

$$\frac{\hbar^2}{m_v^*} = -\frac{\partial^2 E}{\partial k^2} \quad (6)$$

This makes sense because the energy needed to accelerate a hole with velocity zero to a finite velocity is naturally positive. Again, through the energy approximation one can derive the velocity of the holes in the valence band:

$$\vec{v} = -\frac{\hbar(\vec{k} - \vec{k}_{max})}{m_v^*} \quad (7)$$

The effective masses for electrons and holes depend on the curvature of the conduction and valence bands, which rarely match. Therefore, these masses will be different.

Even though the energy gap between bands is what primarily determines if a transition may happen, it is needed to take into account the \vec{k} value where bands lie. If the minimum of the conduction band and the maximum of the valence band have the same \vec{k} value, it is said to have a direct band gap. If that is not the case, the gap is indirect. In the latter case, the hopping electron must have, not only a greater energy than the band gap, but enough momentum to compensate the difference.

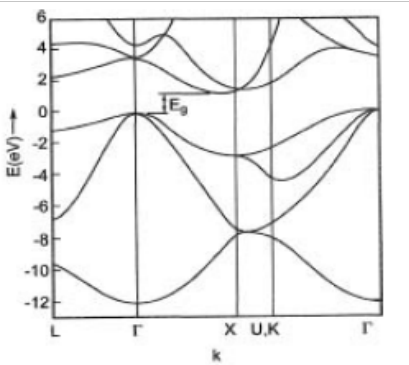


Figure 2: Representation of direct and indirect transitions in silicon (Nelson, 2003).

There are materials used in solar cell physics that undergo indirect transitions as well as direct transitions. To see this we will use the band structure of silicon, which is depicted in figure 2. We notice that the fundamental band gap is about 1,1 eV (Nelson, 2003), but those two points have different values for crystal momentum. This reduces the optical absorption compared to direct gap semiconductors (Nelson, 2003). For this material, direct transitions can happen for electron energies above 3 eV, but those are not useful for photovoltaics (Nelson, 2003).

1.2 Doping Semiconductors. *p-n* Junction

A semiconductor formed by only one type of atom is said to be intrinsic and has no impurities. This is the case considered so far: a semiconductor with a small band gap formed by one type of atom, where the electrons jump from one band to the other by absorbing a photon or by thermal excitations. However, the conductivity of such materials is quite low, since the number of thermal excitations that can happen in an atom is not so great at room temperature. Luckily, it is possible to change the density of carriers by adding impurities to the material, obtaining an extrinsic semiconductor. These impurities are just different atoms from the ones that form the intrinsic semiconductor, so that they create new bonds in the crystal. This process is called doping.

It is easier to understand the effect of impurities in a crystal with an example. Consider an intrinsic semiconductor made of silicon. Silicon has four electrons in its outer level, so it bonds with four different silicon atoms in a covalent bond to form crystal silicon. Now, we introduce several phosphorus atoms in the crystal, in such way that the structure of the material remains unaltered. Since it has one more electron than silicon, when the covalent bond

is formed, the extra electron provided by phosphorus remains unlinked, so it has certain freedom to move around the crystal and thus conduct electricity. Since the material has more density of electrons compared to the intrinsic case, we say it has a type-n doping and that phosphorus is a donor.

Now, consider that the introduced impurity is aluminium, which has one less electron than silicon. Therefore, when the covalent bond is formed with aluminium there is one electron missing and a hole appears, which, analogously to the previous case, can move freely through the crystal. In this case, however, the density of holes has increased compared to the intrinsic case, so the doping is said to be of type-p and that aluminium is an acceptor.

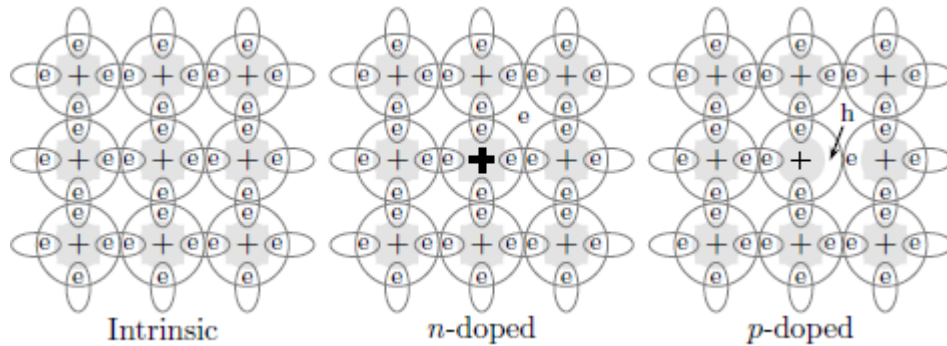


Figure 3: Doping schemes for a silicon semiconductor (Simon, 2013).

It is convenient to have a look at how impurities affect band structure. First, we consider the n-doping situation. The surplus electron behaves like a free electron of effective mass m_e^* , but it is attracted more intensely by the phosphorus atom and the extra proton its nucleus has, so it forms a bound state similar to a hydrogen atom, with two main differences. The first one is that the effective mass of the free electron can be quite different from the bare mass of the electron. Secondly, the two particles attract to each other with a potential given by $V = e^2/(4\pi\epsilon_r\epsilon_0r)$, where ϵ_r is the relative permittivity of the material (Simon, 2013).

With these considerations, one can calculate the energies for the bound state in the crystal. The energy eigenstates for hydrogen atom are given by $E_n = -Ry/n^2$, where Ry is the Rydberg constant given by:

$$Ry = \frac{me^2}{8\epsilon_0^2h^2} \approx 13.6eV$$

with m being the electron mass. The radius of this wavefunction was given in terms of the Bohr radius via $r_n \approx n^2a_0$, where:

$$a_0 = \frac{4\pi\epsilon_0\hbar^2}{me^2} \approx 0.51 \times 10^{-10}m$$

These calculations apply to the impurity bond state, replacing ϵ_0 with $\epsilon_0\epsilon_r$ and the mass m with the effective mass m_e^* . In this way, one obtains:

$$Ry^{eff} = Ry \left(\frac{m_e^*}{m} \frac{1}{\epsilon_r^2} \right)$$

$$a_0^{eff} = a_0 \left(\epsilon_r \frac{m}{m_e^*} \right)$$

Since dielectric constants in semiconductors are usually high and the effective mass is smaller than the regular mass of the electron, the effective Rydberg energy will be smaller than the real one, whereas the effective Bohr radius will be greater. Therefore, the bound state will have an energy just below the conduction band. At low temperatures, this impurity state will be occupied by the corresponding electron, but since its energy is close to the conduction band minimum, it will be very easy for that electron to promote to the conduction band. For a p-doping situation one can carry out a similar calculation and conclude that the impurity adds an empty bound state with energy just above the valence band. In this way, the electrons in the band can be easily excited to occupy the empty states added by the impurity leaving holes behind in the process. Once this analysis has been done, one can conclude that donor impurities increase the number of electrons in the conduction band, while acceptor impurities increase the number of holes in the valence band.

When there are no impurities, the Fermi level of the system lies at the middle of the gap between the valence and the conduction band. Nevertheless, the impurity states modify this parameter, bringing it closer to the conduction band or the valence band depending on whether the doping is n or p , respectively.

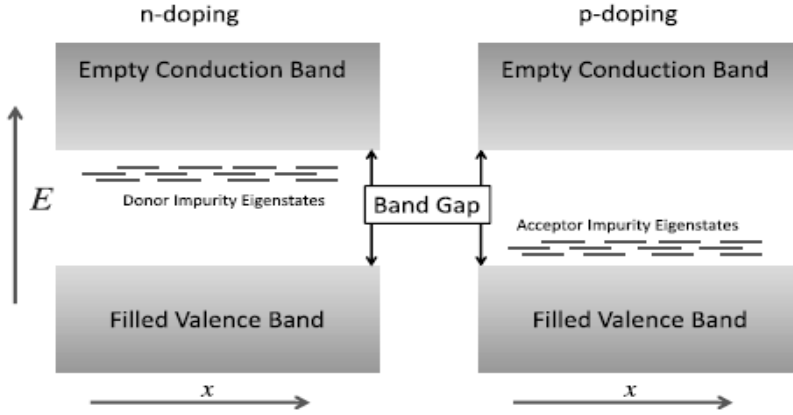


Figure 4: Impurity bound states in n-doping and p-doping situations (Simon, 2013).

Once we have introduced the concept of semiconductor doping and discussed how it affects band structure, we are in a position to understand what happens when a p-doped semiconductor and a n-doped semiconductor are brought together. This is the p - n junction, one of the simplest yet most relevant semiconductor structures.

In the left of the figure 5 are displayed two semiconductors with n and p doping. As already said, the first one has electrons as principal carriers and a Fermi level close to the conduction band, whereas the second has holes as principal carriers and a Fermi energy close to the valence band. When both systems make contact, a carrier migration takes place: holes from the p side travel to the n side and viceversa. As this process goes on, negative and positive ions are left uncompensated, creating a negatively charged region near the p side and a positively charged region near the n side, thus creating an electric field pointing to the negative charges, as shown in the right of the figure 5. This region is called depletion region, since there are no carriers.

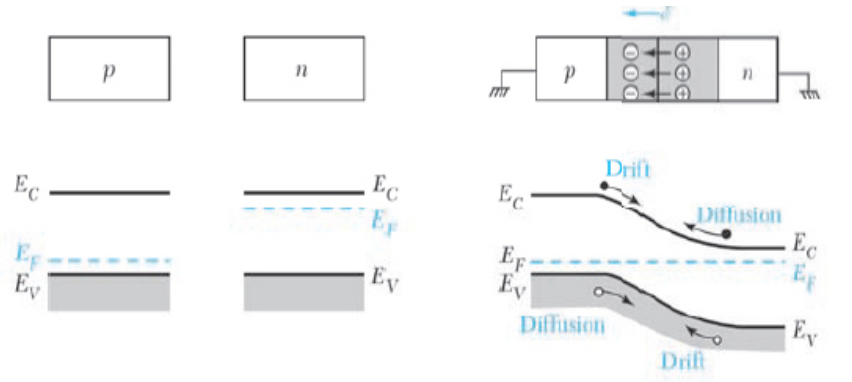


Figure 5: Left: two separate p and n semiconductors. Right: electric field and band diagram of p - n junction (Sze & Lee, 2012)

It is possible to specify the form of the depletion region knowing the impurity distribution via solving the Poisson equation. In this region, where both $p = n = 0$, takes the form (Sze & Lee, 2012):

$$\frac{d^2\psi}{dx^2} = \frac{q}{\epsilon_s}(N_A - N_D) \quad (8)$$

Where N_A and N_D are the negative and positive ions, respectively; ϵ_s is the permittivity of the material and ψ is the electric potential. Concerning how the impurity distribution can be approximated in the junction, two cases will be considered: abrupt and linearly graded junctions.

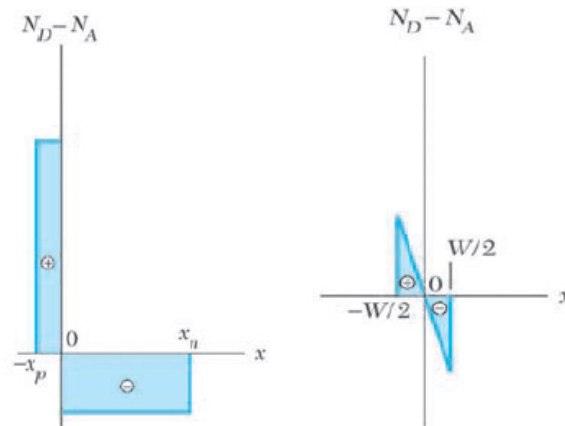


Figure 6: Approximated doping schemes. Left: abrupt junction. Right: linearly graded junction. (Sze & Lee, 2012)

In the abrupt junction, the Poisson equation is simplified to:

$$\frac{d^2\psi}{dx^2} = \frac{qN_A}{\epsilon_s} \text{ for } -x_p \leq x < 0, \quad (9)$$

$$\frac{d^2\psi}{dx^2} = -\frac{qN_D}{\epsilon_s} \text{ for } 0 < x \leq x_n \quad (10)$$

Where x_p and x_n are the widths of the p and n contributions in the depletion region. Therefore, the total width of the depletion region is given by $W = x_n + x_p$. The electric field is obtained integrating equations (9) and (10):

$$E(x) = -\frac{qN_A(x+x_p)}{\epsilon_s} \text{ for } -x_p \leq x < 0, \quad (11)$$

$$E(x) = \frac{qN_D(x-x_n)}{\epsilon_s} \text{ for } 0 < x \leq x_n \quad (12)$$

Integrating equations (11) and (12) over the depletion region gives the total potential variation (Sze & Lee, 2012), known as built in potential:

$$V_{bi} = -\int_{x_p}^{x_n} E(x)dx = \frac{qN_A x_p^2}{2\epsilon_s} + \frac{qN_D x_n^2}{2\epsilon_s} \quad (13)$$

Taking into account that the total negative space charge in the p area must be equal to the total positive space charge in the n area:

$$N_A x_p = N_D x_n$$

We combine the previous equations and write the depletion region width in terms of the built in potential:

$$W = \sqrt{\frac{2\epsilon_s}{2} \left(\frac{N_A + N_D}{N_A N_D} \right) V_{bi}} \quad (14)$$

This derivation has considered thermal equilibrium and no polarization, but it is worth to take a look at what happens when an external potential is applied. On the one hand, if a positive potential V is applied to the p side, the junction becomes forward biased and the total electrostatic potential is decreased by V . On the other hand, if the same positive potential is applied to the n side, then the junction becomes reverse biased and the total potential is increased by V . This way, one can easily reach the conclusion that forward bias reduces the depletion region width, and vice versa. In particular:

$$W = \sqrt{\frac{2\epsilon_s}{2} \left(\frac{N_A + N_D}{N_A N_D} \right) (V_{bi} - V)} \quad (15)$$

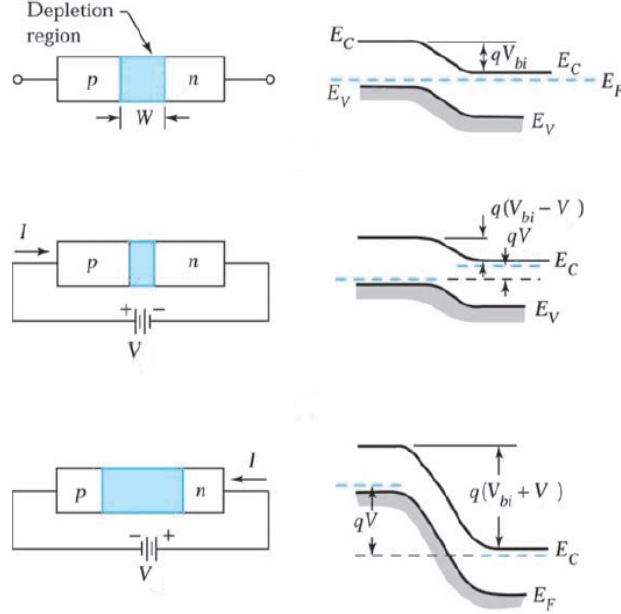


Figure 7: Effects of biasing in depletion region width. Top: unbiased junction. Center: forward bias junction. Bottom: reverse bias junction. (Sze & Lee, 2012).

For a linearly graded junction, the Poisson equation for the potential can be written as:

$$\frac{d^2\psi}{dx^2} = -\frac{q}{\epsilon_s}ax \quad , \quad -\frac{W}{2} \leq x \leq \frac{W}{2} \quad (16)$$

Where a is the impurity gradient. We can find the electric field by integrating equation (16), taking into account that there is no electric field at $x = \pm \frac{W}{2}$, obtaining:

$$E(x) = \frac{qa}{\epsilon_s} \left[\frac{(W/2)^2 - x^2}{2} \right] \quad (17)$$

Integrating now equation (17) we find the built in potential:

$$V_{bi} = \frac{qaW^3}{12\epsilon_s} \quad (18)$$

And, in terms of this parameter, the depletion layer width:

$$W = \left(\frac{12\epsilon_s V_{bi}}{qa} \right)^{1/3} \quad (19)$$

When an external potential is applied to a linearly graded junction one obtains the same results and conclusions shown in equation (7), but now the depletion layer width varies with $(V_{bi} - V)^{1/3}$, with V being positive for forward bias and negative for reverse bias.

After this analysis has been made, it is possible to conclude that p - n junctions can be modeled as diodes, regarding how voltage and current behave in the junction. Specifically, when a positive voltage is applied to the p side respect to the n side, a current flows in this direction proportional to the magnitude of the voltage. This case corresponds to a forward biased diode. On the contrary, when the polarity of the voltage is reversed, there is a current flowing in the n - p direction, but it is so little that it can be neglected. This is the case for a reverse biased diode (Prat, 1999).

The most appropriate way to model this kind of diodes is via the exponential model, which relates current and voltage through an exponential relation:

$$I = I_S \left(e^{qV/kT} - 1 \right) \quad (20)$$

□

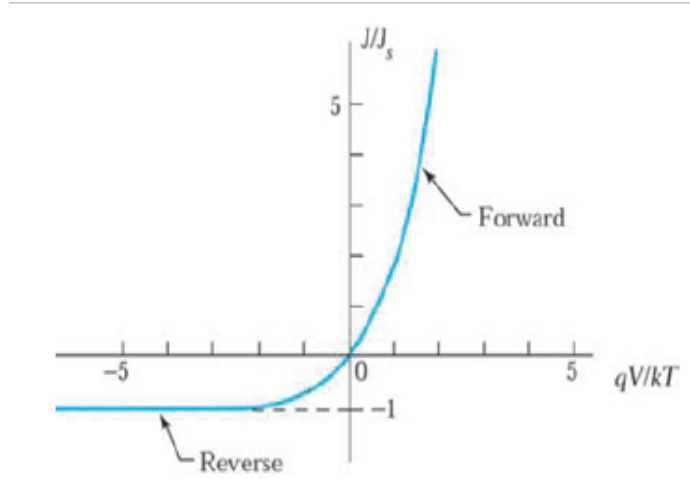


Figure 8: Current-Voltage diagram for a diode (Sze & Lee, 2012)

1.3 *p-n* Junctions under solar irradiation. Solar cells efficiency principles.

Solar cells are devices capable of generating power when exposed to solar irradiation. They are made of a semiconductor material, generally silicon, whose electrons can be excited by photons of solar light to hop from one band to another. Specifically, when an incident photon has lower energy than the band gap E_g it has no effect in the solar cell, while photons with energy above the band gap contribute with E_g to the solar cell output while the surplus energy is lost as heat. The potential in the depletion region depends on the built-in potential, which in turn depends on the band gap. For this reason, the current decreases as the band gap increases.

We now seek to find the efficiency of energy conversion of solar cells. First, the energy coming from the Sun that reaches the atmosphere is known as solar constant and has a value of 1367 W/m^2 . This energy is scattered when crossing the atmosphere, depending on the length of the path that light travels.

Under solar irradiation, it is convenient to derive the I - V characteristics of the cell using its equivalent circuit, which is the same as a diode. In figure (9), I_L is the current due to the solar excitation, I_S is the saturation current of the diode and R_L is the load resistance.

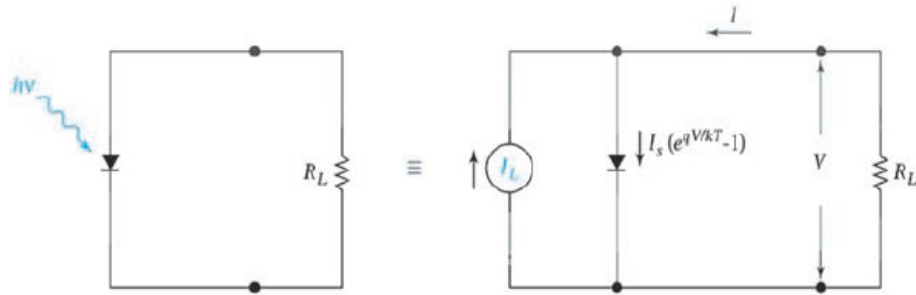


Figure 9: Equivalent circuit of a solar cell (Sze et al., 2012).

In this case, the ideal I - V characteristics are given by:

$$I = I_S \left(e^{qV/kT} - 1 \right) - I_L \quad (21)$$

When equation (21) is used to plot voltage against current, one obtains the curve shown in figure (10). Through this diagram one defines I_m and V_m as the values of current and voltage that maximise the power output of the cell, which is given by $P_m = I_m V_m$.

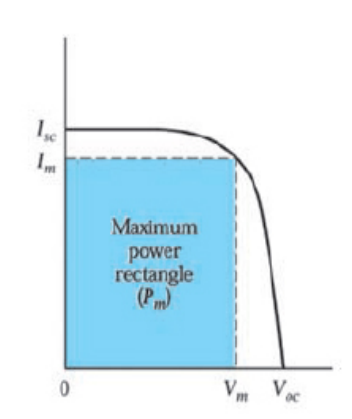


Figure 10: I-V curve for a solar cell, with its rectangle of maximum power (Sze & Lee, 2012).

Through equation (21) one can obtain the open circuit voltage:

$$V_{OC} = \frac{kT}{q} \left(\frac{I_L}{I_S} \right) \quad (22)$$

The condition for maximum power is $dP/dV = 0$, which gives:

$$V_m \approx V_{OC} - \frac{kT}{q} \ln \left(1 + \frac{qV_m}{kT} \right) \quad (23)$$

$$I_m \approx I_L \left(1 - \frac{1}{qV_m/kT} \right) \quad (24)$$

This way, the maximum power is:

$$P_m \approx I_L \left[V_{OC} - \frac{kT}{q} \ln \left(1 + \frac{qV_m}{kT} \right) - \frac{kT}{q} \right] \quad (25)$$

The ideal efficiency of a solar cell is defined to be the ratio between the maximum power and the incident power, namely:

$$\eta = \frac{I_m V_m}{P_{in}} = \frac{FF \cdot I_{SC} V_{OC}}{P_{in}} \quad (26)$$

Where we are considering $I_L \approx I_{SC}$. FF is the fill factor, which depends only on values of current and voltage of the circuit. It is defined as:

$$FF = \frac{I_m V_m}{I_{SC} V_{OC}} \approx 1 - \frac{kT}{qV_{OC}} - \frac{kT}{qV_{OC}} \ln \left(1 + \frac{qV_m}{kT} \right) - \frac{kT}{qV_{OC}} \quad (27)$$

To maximise efficiency, one seeks to maximise the maximum values of voltage and current and the fill factor. There are a lot of factors that decrease efficiency,

like the irradiation lost due to reflection in the surface of the solar cell. The ideal maximum efficiency is therefore 31% (Sze & Lee, 2012).

2 Solar Pump Installation

2.1 Contextualization of the Installation

Before the modelling and the installation of the solar pump, it is necessary to provide some information and context about the villages where the solar pumps were installed and the people who are benefiting from it. Two installations have taken place in two nearby villages in the region of Dioulacolon, named Darou and Sampathé, in southern Senegal. Those villages share very similar characteristics in terms of their ethnic groups or living conditions.

The modelled installation in this work corresponds to the one carried out in Sampathé. Since this population is located within a large baobab forest, the road communication is poor, and thus they do not have easy access to electricity or current water. The predominant ethnic group is Peul, majority in western Africa but not in Senegal, and they are known to be traders, nomads and great livestock farmers. They practice polygamy where wives move to the family home of their husbands, on whom they depend. It is common to find families where the husband is absent, either because he tries to get better job opportunities in other cities or countries, or because he abandons his family. Moreover, the female schooling level is level in rural regions due to the tasks they are required to do on a daily basis, so women do not have means to live on their own. However, these women are conscious about their situation and they fight so their daughters do not have to live like they do. This desire has encouraged them to form women associations to engage in economic activities and gain some financial freedom that allows them to keep their children in school.

One of the most efficient ways they have found to improve their economy is to farm and sell vegetables when it is not the season to grow rice, the main crop of the country. Community farms are set up, where each women is responsible for their part. Since there is not current water in Sampathé, these crops are irrigated with water extracted from boreholes. They carry this water from the borehole to the farm several times a day and repeat it as many times as necessary to properly irrigate the crops. This is an extremely exhausting process by itself, without considering the other duties expected from women, like cooking or taking care of the children.

For this reason, the most requested solution in cooperation projects is a system that allows them to extract water from the borehole without the physical effort and the time they put in. With that in mind, the cooperation project between the village and the *Universidad de La Laguna* consisted in the installation of a solar bomb to put a solution to this problem.

2.2 Description of the Installation

In general terms, solar pumps can be located above the ground or within the water, depending on the water source. The first systems are used when the water source is a shallow well or a lake: the pump is located above the water level and a suction pipe is used to draw water from the source. In this case, however, the water source is a borehole, so we need to use a submersible pump. In this case, the solar array and the pump controller are typically located near the top of the borehole, connected to the submersible pump through waterproof cables. This type of installation also requires a sensor measuring the water level constantly, in order to prevent the pump to function when there is not enough water.

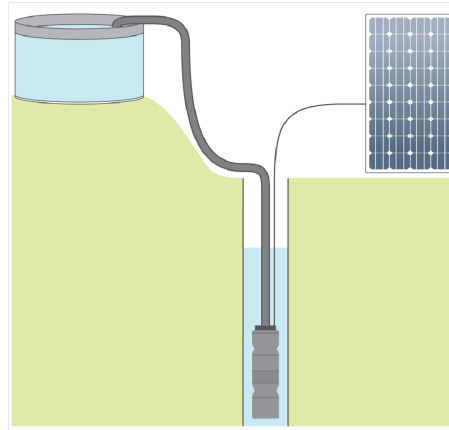


Figure 11: General scheme of a submersible solar pump.

According to the requirements of the final users, a total of four basins of $3 m^3$ of capacity are needed. The basin destined to provide water for livestock ($B1$) is located six metres ($6 m$) away from the borehole; and the basin meant for horticulture ($B2$) is thirty five metres ($35 m$) away. The basin $B2$ provides water to two other basins ($B3$, $B4$), at negligible distance from $B2$.

Water is carried from the borehole to two mini-basins ($MB1$, $MB2$) before being finally deposited in the main basins $B1$ and $B2$. The scheme for the installation that will be followed here is represented in the next diagram:

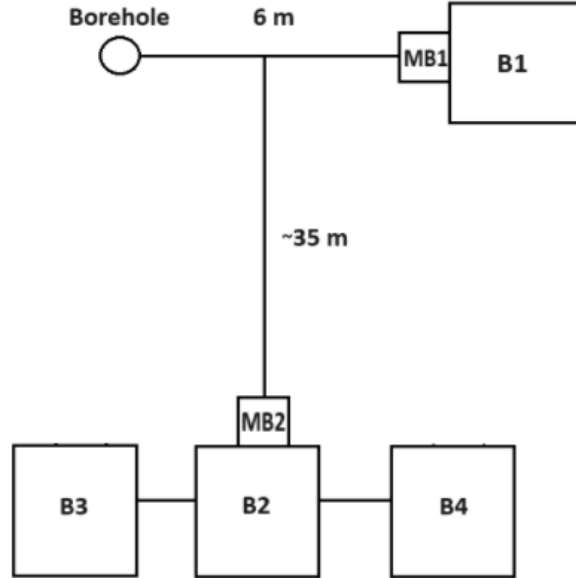


Figure 12: Disposition of the different elements of the installation.

The water needs of the community have been estimated at sixty cubic metres per day ($60 \text{ m}^3/\text{day}$) to facilitate the adequate growing of the crops and ensure the livestock is properly hydrated.

First of all, it must be specified which which type of water pipe we will be using for the installation. Water pipes are usually supplied as galvanized iron pipes, PVC pipes and polyethylene (PE) pipes. The first type is not recommended in this situation, as it has a slightly rough interior which causes higher friction losses than plastic pipes. Also, metal pipes will eventually rust and they will have to be changed. Both PE and PVC pipes could be selected for the installation as they have similar characteristics, but in the following we will be considering the PVC pipe because it is preferable for potable water, even though it needs to be protected from solar radiation via UV blocking paint to prevent discoloration or cracks.

The first thing we need to obtain is the electrical needs per day, which is given by:

$$E_1 = \frac{V \cdot TH \cdot 2,725}{PPR} \quad (28)$$

Where E_1 is the daily electrical energy, V is the water volume measured in cubic metres per day, TH is the total head measured in metres and PPR stands for pump performance ratio. As it was stated before, the water volume is $60 \text{ m}^3/\text{day}$; and the pump performance ratio will be fixed to unity. The total

head is the measurement from the bottom of the borehole to the final destination of the water, taking into account the friction losses in the pipes as metres of water column. The largest distance that water will have to travel is the distance from the borehole to the basin *B2*, which has a first section of three metres long connected to a T-shaped joint followed by a thirty-five metres section. There are several formulas to calculate the friction losses in water pipes, but we are going to use the Hazen-Williams expression, as it is commonly used in potable water pipes (Henares, 2023). It is written as:

$$H = 10,67 \cdot \frac{Q^{1,85}}{C^{1,85} \cdot D^{4,87}} \quad (29)$$

where H is the friction loss in metres of water column, Q is the flow rate through the pipe in cubic metres per second, D is the internal diameter of the pipe and C is the Hazen-Williams coefficient, which is $C = 150$ for a PVC pipe. This way we can obtain the friction losses associated with each section:

Section	Flow rate (m^3/s)	Diameter (mm)	H (m)
<i>a</i>	$2,77 \cdot 10^{-3}$	65	0,03
<i>b</i>	$1,39 \cdot 10^{-3}$	65	0,11

Here, we have considered that the flow rate divides at half when crossing the T-joint and we have selected an internal diameter of 65 *mm* for the pipes so the losses are minimum. Furthermore, we have to add the equivalent length coming from the T-joint, which is 0,40 *m*. With all of this, we can finally calculate the total head as the sum of every length listed here plus the borehole depth and the basins height:

$$TH = 8 + 1 + 35,11 + 3,03 + 0,40 = 47,54 \text{ m} \quad (30)$$

Now, the electrical needs are given by:

$$E_1 = 60 \cdot 47,54 \cdot 2,725 = 7772,79 \text{ Wh/day} \quad (31)$$

The rated power of the pump is just the fifth part of the daily electrical needs:

$$P_1 = \frac{E_1}{5} = \frac{7772,79}{5} = 1554,56 \text{ Wh/day} \quad (32)$$

In this case, we want the pump to be powered by solar cells, so it is needed to calculate the total required power of the solar panels, given by:

$$Wp = \frac{E_1 \text{ (Wh/day)}}{I \text{ (kWh/day/m}^2\text{)} \cdot PR} \quad (33)$$

Where I is the daily irradiance and PR is the performance ratio. This value depends on the type of installation and the operating conditions; in this case we are going to take $PR = 0,6$. The daily irradiance value has been estimated

as $I = 6,38kWh/m^2/day$, according to free data from the European Commission (annex A). The data has been taken from the city of Kolda, which is some kilometres away from Sampathé, but has similar values in terms of irradiance. With this data, the total required power from the solar panels is:

$$Wp = \frac{7772,79}{6,38 \cdot 0,6} = 2030,51 Wp \quad (34)$$

The number of solar panels that are needed to supply this energy demand depends on the rated power of the solar panels: some options are shown below:

Nominal power (W)	Number of panels	Peak power (W)
300	7	2100
350	6	2100
410	5	2050

Among these options, the one which is most suitable according to the installation characteristics is to install six solar panels of 350 W of rated power to meet the energy demand.

To finish the dimensioning, it is needed to find a pump that matches the energy calculations done in this section. This research has been made using the *Grundfos sizing page*, that looks for the most appropriate pumps according to the total head, the flow rate and the type of installation. Two options have been found to be the best choices: SPE 18-12 and SPE 18-8 models. Both are suitable for extracting current water from the borehole and are capable of transporting water to where it needs to be deposited while working at a decent performance ratio. The SPE 18-12 model is a slightly better fit, as its maximum energy requirement is lower than that produced by the solar cells, which is not the case for the SPE 18-8 model. Comparing with the actual installation, which information is provided in *Annex B*, we see that the actual pump and the SPE 18-12 model have similar current operating points.

Type	SPE 18-12	Type	SPE 18-8
Quantity * Motor	1 * 7.5 kW,	Quantity * Motor	1 * 5.5 kW,
Flow	10 m ³ /h	Flow	10 m ³ /h
H total	47 m	H total	47 m
Power P1	2.096 kW	Power P1	2.202 kW
Power P2 required in the duty point	1.664 kW	Power P2 required in the duty point	1.736 kW
Current (rated)	16.6 A	Current (rated)	12.6 A
Current (actual)	5.2 A	Current (actual)	5.2 A
Cos phi (actual)	0.59	Cos phi (actual)	0.61
Eta pump	76.8 %	Eta pump	73.6 %
Eta motor	79.4 %	Eta motor	78.8 %
Eta total	61.0 % =Eta pump * Eta motor	Eta total	58.0 % =Eta pump * Eta motor
Speed	65 %	Speed	77 %
Speed	1943 rpm	Speed	2295 rpm
Flow total	36317 m ³ /year	Flow total	36317 m ³ /year
Spec. energy consumption	0.2088 kWh/m ³	Spec. energy consumption	0.2196 kWh/m ³
	4.44 Wh/m ³ /m		4.67 Wh/m ³ /m
Energy consumption	7620 kWh/Year	Energy consumption	8014 kWh/Year
CO2 emission:	4340 kg/Year	CO2 emission:	4570 kg/Year
Price	On request	Price	On request
Life cycle cost	26353 EUR /10Years	Life cycle cost	24641 EUR /10Years

Figure 13: Technical characteristics of SPE 18-12 and SPE 18-8 models, respectively.

3 Challenges of International Cooperation

International cooperation projects are less effective than they may seem to be, as countries where a lot of effort and money is invested do not appear to be much more developed after the cooperation. There are a number of reasons that can explain why this happens.

On the one hand, there is a cultural shock between the local population and the cooperators, which does not take place in equality between the parts. The local populations know that they have to give in to our way of doing things in order to get the help we offer, even though most of the time we do not take into account their way of life or their customs. For a long time it has been thought that these societies were not able to develop for themselves and the help that came provided them with things we thought they needed, but not necessarily what they wanted. In any case, this type of relationship can hardly be seen as cooperation.

On the other hand, the NGOs normally face difficulties to get their cooperation projects founded and approved. At least in Spain, it is much more important to know what is going to be done and how much it costs rather than what is the methodology to follow or the relationship with the local population,

even though this is what will ultimately determine if the project has a real effect or not. However, NGOs know that it is better to provide *some*, maybe deficient, help; rather than to *not* help, so they tend to accept projects they know they can carry out even if they do not have the correct approach.

However, this has not been the case for this project. The solar pump is a severe improvement in the living conditions of these women while improving the performance of the farm, which in turn provides them with more financial possibilities. The NGO is in constant touch with the population benefiting from the installation to make sure everything works as it should. And the village population did their part too, which consisted in building the basins where water was meant to be deposited, weeding the zone and lifting up protections so that the solar cells could be protected from animals. This is proof that there is a paradigm shift on the way things work regarding international cooperation. The fact that this reflection can happen and that I too know why the solar pump has been installed instead of anything else demonstrates that this international cooperation project has the correct approach and has been carried out as it should.

4 References

Sze, S. M., & Lee, M. K. (2012). *Semiconductor Devices: Physics and Technology, 3rd Edition*. Wiley.

Nelson, J. (2003). *The Physics of Solar Cells*. Imperial College Press.

Simon, S. (2013). *The Oxford Solid State Basics*. Oxford.

Prat, L. (1999). *Circuitos y dispositivos electrónicos. Fundamentos de Electrónica*. UPC.

(2023, 29 de junio). Pérdida de carga en tuberías. *Desatascos Henares*.
https://re.jrc.ec.europa.eu/pvg_tools/es/

5 Annexes

A. Monthly and Yearly Solar Irradiation in Kolda

PVGIS-5 geospatial irradiance database. Data provided:

- Latitude/longitude: 12.891/-14.938
- Horizon: calculated
- Database: PVGIS-SARAH2
- Initial year/final year: 2020/2020
- Included variables in this report: global horizontal irradiation, normal direct irradiation, global irradiation at the optimum angle.

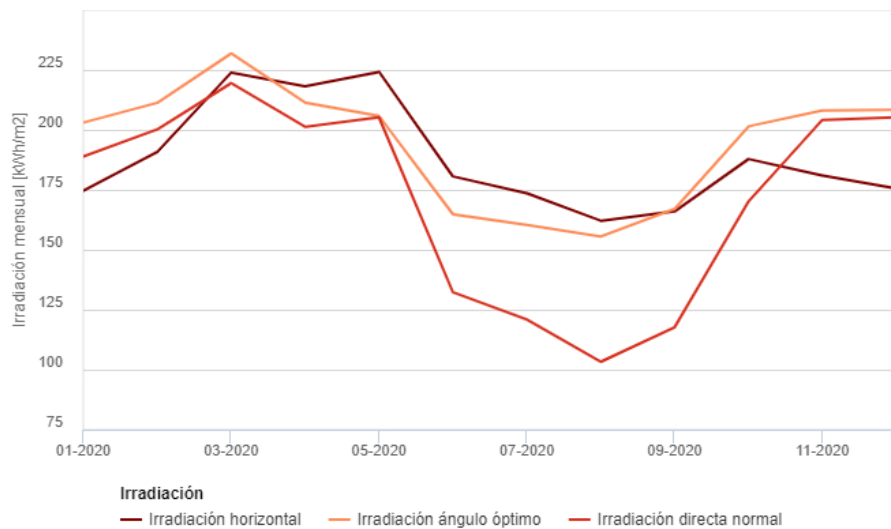


Figure 14: Graphic of monthly solar irradiation in Kolda

Month	Global horizontal irr.	Direct normal irr.	Optimal angle irr.
January	174,67	188,94	203,07
February	190,87	200,21	211,28
March	223,84	219,48	231,86
April	218,20	210,32	211,42
May	224,18	205,20	205,83
June	180,60	132,29	164,81
July	173,56	120,92	160,41
August	162,12	103,28	155,53
September	165,99	117,64	167,03
October	187,86	170,22	201,48
November	180,99	204,17	208,11
December	175,51	205,29	208,39

Table 1: Global horizontal, direct normal and optimal angle irradiation, measured in kWh/m^2 .

B. Information Provided by the Installation Company

Sampathé is a village located about six kilometers away from Kolda, in the south of Senegal. Our mission is to install a solar pumping system to facilitate access to water for the horticulture activities of a group of women.

It is a one-hectare market garden. In the place it was found a single borehole of eight metres depth, along with two principal basins, one for livestock (three cubic metres) and another one feeding three other three-cubic metres basins used for horticulture. Their daily needs are estimated in sixty cubic metres per day.

A solar pump of ten cubic metres per hour of flow rate has been installed, fueled by four solar panels of 350 W each.

1. Daily and weekly water needs: It has been estimated in 100 cubic metres per day, 700 a week.
2. Distance between the borehole and the basins: Each basin is one metre high and has a volume of three cubic metres. The livestock basin is six metres away from the borehole and the horticulture basin is thirty five metres away.
3. Static components of the pump: 1100 W of rated power, 72 V tension DC, 16 A current DC, 10 m^3/h of flow rate, 65 m of maximum distance.
4. Monthly and yearly solar irradiation: To calculate from the facilitated data.
5. Maximum flow rate to calculate dynamic head: 10 m^3/h .
6. Information about the solar panels manufacturer: property of Asaman Solar Power Center.
7. Electric wire length: 5 m between panels and controller, 13 m between pump and controller, 11 m between the probe and the controller.
8. Pipe parameters: PVC pipe to protect the wires: 5 m of pipe for the distance pump-controller and another 5 m for the distance panels-controller.

Joint pressure pipes between the basins and the pump: The joint pipe connecting the pump to the mini-basins to allow water to escape is 10 metres long.

The pump fuels directly two mini-basins through a T-shaped joint of diameter 32 and two pressure valves of diameter 32. One of the mini-basins is connected to the big basin reserved for livestock and the other one is connected to another big basin, which fuels another two basins for horticulture activities thanks to a system of pipes in the place.

Flow rate for each pool: 5 cubic metres per hour thanks to our T, which divides the water coming from the pump into 2.

C. Photographs of the Farm and the Solar Pump System



Figure 16: Installation of solar panels



Figure 17: Structure of the borehole



Figure 18: Crops



Figure 19: International cooperation